

## Article

# Adaptation and Validation of Injection Rate Predictive Model for Solenoid Type Injectors with Different Nozzle Geometry

Edgar Vicente Rojas-Reinoso <sup>1</sup>, Karen Morales-Chauca <sup>1</sup>, Jandry Lara-Lara <sup>1</sup>, José Antonio Soriano <sup>2</sup>  
and Reyes García-Contreras <sup>2,\*</sup>

<sup>1</sup> Grupo de Ingeniería Automotriz, Movilidad y Transporte (GiAUTO), Carrera de Ingeniería Automotriz-Campus Sur, Universidad Politécnica Salesiana, Quito 170702, Ecuador; erojas@ups.edu.ec (E.V.R.-R.); kmoralesc4@est.ups.edu.ec (K.M.-C.); jlaral1@est.ups.edu.ec (J.L.-L.)

<sup>2</sup> Instituto de Investigación Aplicada a la Industria Aeronáutica, Escuela de Ingeniería Industrial y Aeroespacial, Universidad de Castilla-La Mancha, Av. Carlos III, s/n, 45071 Toledo, Spain; joseantonio.soriano@uclm.es

\* Correspondence: mariareyes.garcia@uclm.es

**Abstract:** The present research analyses the injection rate of a direct rail injection diesel engine, focusing specifically on the influence of the nozzles and various operating conditions from real road tests on the rate of injection. A diesel injector test bench was used for feedback with real data from the test vehicle under real road conditions. An analysis of the behaviour of the injection rate was carried out using the zero-dimensional model. This model generated a predictive model that incorporated the five variables identified through a developed multivariate analysis of variance, showing a high correlation of dependence between variations in injection pressure, the diameter of the holes, and the number of holes with greater representativeness. The results obtained showed that the nozzle geometry and the physical properties of the fuel had a direct effect on the injection rate. This analysis enriches the understanding of fuel injection and its effects on diesel engine performance by providing an analysis of the system components that influence the injection rate and generating a simple tool to feed thermodynamic diagnostic models. The proposal model may be used as an input in thermodynamics predictive models and reduce the simulation load in computational fluid dynamics predictive models.

**Keywords:** diesel injection; fuel mass rate; zero-dimensional model; nozzle geometry; volumetric fuel flow



**Citation:** Rojas-Reinoso, E.V.; Morales-Chauca, K.; Lara-Lara, J.; Soriano, J.A.; García-Contreras, R. Adaptation and Validation of Injection Rate Predictive Model for Solenoid Type Injectors with Different Nozzle Geometry. *Appl. Sci.* **2024**, *14*, 3394. <https://doi.org/10.3390/app14083394>

Academic Editor: Jun Cong Ge

Received: 8 March 2024

Revised: 11 April 2024

Accepted: 15 April 2024

Published: 17 April 2024



**Copyright:** © 2024 by the authors. Licensee MDPI, Basel, Switzerland. This article is an open access article distributed under the terms and conditions of the Creative Commons Attribution (CC BY) license (<https://creativecommons.org/licenses/by/4.0/>).

## 1. Introduction

The automotive industry has been researching and trying to optimize the performance of and reduce the fuel consumption in internal combustion engines for years [1–3], with the aim, among others, of obtaining greater energy use by the engines. At the same time, there is a need to control harmful emissions that are released into the environment, which has led to the creation of increasingly strict regulation standards [4,5]. Vehicles powered by compression ignition engines are the most used for transporting goods. Diesel engines are the most common in heavy-duty machinery [6] because of their great fuel economy and the torque they give to the engine [7,8]. For this reason, the goal of reducing pollutant emissions while performance is optimized has become an important mission, upon which various studies such as the one that will be developed below are based [9].

Unlike a spark ignition engine, in compression ignition engines, the distribution of fuel inside the chamber is a key factor that allows for controlling the quality of combustion [10]. For this reason, a multitude of parameters can be modified to control injection in a diesel engine, including the injection pressure, fuel flow, air temperature, injector spray angle, injector geometry, and combustion chamber [11]. All this is summarised in the control of the injection rate, which allows one to obtain more out of the fuel used and reduce the range of pollutant emissions [12,13].

The geometry of the nozzle is a determining factor in varying the behaviour of the injection rate curve [14,15]. Nozzle geometry refers mainly to existing variations in size, length, taper, and the number of holes [16]. Its arrangement on the body and the shape of the tip allows for control of fuel atomization, jet distance, injection angle, fluid turbulence, and injected quantity [17]. On the other hand, the minimum changes in the injection rate curve do not represent significant variations in combustion [18–20]. However, the atomization of the fuel and the distance reached by the injected jet will present differences in turbulence, in addition to generating a greater homogeneity with the oxidizer, allowing for greater control of the emissions and fuel used. The injection rate of a diesel engine can be determined by various experimental methods and computer models, as indicated in the review of C. Mata et al. [21], where the 0D, 1D, 2D, 3D, and multidimensional techniques for determining the diesel injection rate are compiled and described. However, modelling injection rates does not require the same amount of quantitative data (depending on the complexity of the model), 1D models require the use of advanced computational tools [22], and for more advanced models, even artificial intelligence training based on the repetition of results is needed. Due to the simplicity of 0D models, a simple model is proposed for determining the rate of injection, fuel mass flow, and/or volumetric flow of fuel.

The modelling of the 0D injection rate focuses on the measurement and control of physical variables obtained from the injected fuel, which do not require very advanced computational elements and, consequently, facilitate their measurement and allow for calculations to be made in real time [18]. Fluid dynamics properties are also applied in modelling [23], so it is necessary to know some properties of the fuel used [24]. Typical variables measured with this technique are fuel flow, fluid mass, and nozzle geometry. Modifications in the injection pressure also show significant changes in the injection curve [25].

Zero-dimensional modelling, due to its versatility and low complexity at the level of data acquisition and processing, facilitates optimal configuration when tuning automobile injection [26], because it allows the search and modifications of the parameters to obtain a better result in terms of energy and consumption. This is a key difference from the rest of the models, which are more complex and require much more time to develop [21].

In this study, the objective is to show that the geometry of the nozzle and the number of holes play important roles in shaping the behaviour of the injection curve, as has already been demonstrated in previous works, and apply this to real operating conditions [27]. Through extensive analysis, the quantitative and qualitative relationships between specific nozzle geometries and orifice numbers are evaluated, and their influence on the intensity and consistency of spray velocity is assessed. The results obtained from this work will provide a greater understanding of the injection process, with important implications for the design and optimization of systems related to this fundamental process in combustion engines.

Additionally, a theoretical–experimental and statistical study is presented to recognize how the injection rate varies by changing the geometry of the nozzles in a solenoid-type injector. The range of pressures and engine regimes selected for this study (highway driving cycle [28]) are representative of the work conditions of the 4JJ1 Diesel engine, where this type of injector is equipped. This range was used to obtain the injection rate curve using the 0D model using two types of fuel (conventional diesel and fuel used to calibrate injectors and injection pumps called Viscor). Furthermore, it should be noted that the Isuzu D-max 3.0 CRDI pick-up vehicle, which is powered by the engine chosen for the development of this study, is one of the most marketed models in Central and South America [29]. In this way, the importance of optimizing fuel use is highlighted to increase vehicle efficiency.

Although the proposed modelling is not predictive of the shape of the point-to-point fuel injection rate, this model can be used as an input to predictive thermodynamics models and reduce the simulation load in predictive computational fluid dynamics models.

## 2. Materials and Methods

### 2.1. Materials

To have proper control of the fuel injection process during the highway driving cycle, it is necessary to know the engine operating parameters (engine speed, timing of injection, and pressure of injection) of the Isuzu 4JJ1 engine. To achieve this, an online data acquisition and analysis system will be implemented using the PAD V Launch equipment and a Micsig mini TO1104 oscilloscope. These tools allow to collect data on the fuel delivered to the combustion chamber. Tables 1 and 2 show how to use the equipment characteristics, including the injector activation time and injection pressure, under different working conditions. This analysis covers all operating conditions from an idle to full engine load.

**Table 1.** Vehicle characteristics.

Brand	Model	Engine	Fuel	Cylinder	Cylinder Number
Isuzu	D-max	4JJ1 CRDI	Diesel	3.0 L	4

**Table 2.** Equipment characteristics.

Equipment	Brand	Model
Scanner	Launch	X-431 PAD V
Laptop	Dell	G3
Oscilloscope	Missing	tBook mini TO1104
Amperometric clamp	Fluke	362

Once the vehicle data are obtained under real operating conditions, they will be transferred to an injection diagnostic bench, in which the values of injection pressure, operating voltage, injector energization time, injection pulse width, injection frequency, and the angular speed of the high-pressure pump are modified according to the performance characteristics of the 4JJ1 engine. Flow data will be collected for each injection. Once the flow rates and injection volume are tabulated, a gravimetric balance is used to verify the value of the mass of fuel delivered by each activation of the injector. These variables will allow the injection rate to be calculated.

To check that the injector works under identical operating conditions to those in the real vehicle tests, the injection pressure, energizing time, injector voltage, amperage, and operating temperature will be recorded using a current clamp and oscilloscope. These tests are carried out with 4 injectors, whose geometries are the most used in the study area in the different pick-ups. Figure 1 shows the scheme of the work methodology and the definition of each number is included in Table 3.

**Table 3.** Detail numbers Figure 1.

Number	Denomination
1	Diesel injector test bench
2	Electronic Control Unit
3	Injection pump
4	Common Rail
5	Injector
6	Nozzle
7	Clamp meter
8	Oscilloscope
9	Beaker
10	Gravimetric balance
11	Personal Computer

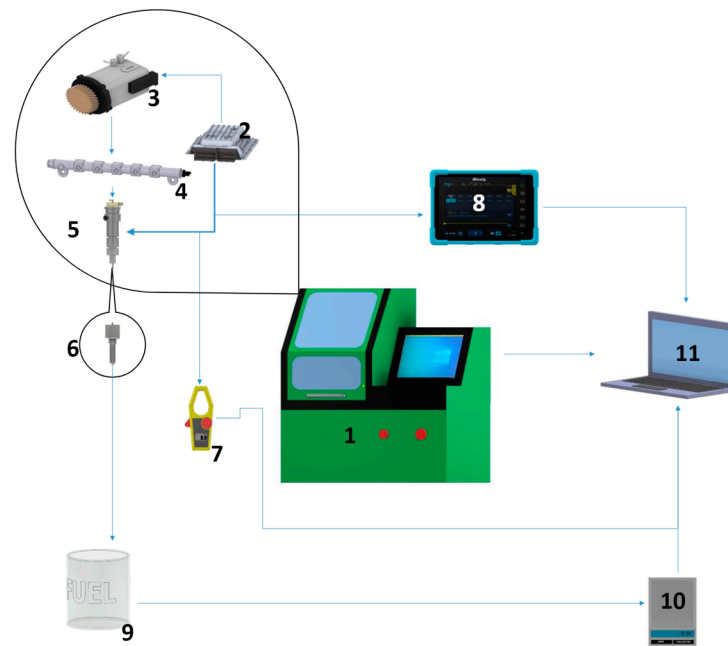


Figure 1. Work flowchart.

The characteristics of the fuel greatly influence the injection behaviour. Properties such as density, viscosity, and injection system (such as pressure and temperature) influence the characteristics of the hydraulic movement of the injector (they circulate with more or less difficulty within a hydraulic circuit). In turn, these properties affect the degree of atomization and, therefore, the air–fuel mixture that will take place in the cylinder. To study the influence of fuel in this work, two fuels were used, whose physico-chemical properties are detailed in Table 4.

Table 4. Characteristics of the fuels used.

Denomination	Fuel 1	Fuel 2	Units
Commercial designation	Viscor 1487 AW-2	Diesel	-
Density	780	850	[kg/m <sup>3</sup> ]
Viscosity kinematics at 40 °C	2.62	4.1	[mm <sup>2</sup> /s]
Kinematic viscosity at 100 °C	1.07	1.9	[mm <sup>2</sup> /s]
Kinematic viscosity at 20 °C	102	52	[mm <sup>2</sup> /s]

Viscor 1487 AW-2 fuel is a fuel fluid that is used to calibrate injection pumps and injectors, so it was used to calculate the injection rate, since, with this fuel, one can know the real operation of the injector and how it behaves with different nozzles according to the manufacturer's characteristics. On the other hand, diesel was used, because it is the typical fuel used in compression ignition engines.

## 2.2. Methodology

To obtain the specific data for controlling the fuel injection in the vehicle, a straight, unslipping paved road with an extension of 4 kilometres was chosen, located at an approximate elevation of 2411 m above sea level (masl). A normal driving cycle was implemented, respecting the speed limit established by local traffic regulations. From these tests, specific values of injection pressure and injector activation time were obtained from idle (695 min<sup>-1</sup>) to maximum engine load, which was reached at an engine speed of 3000 min<sup>-1</sup>. The values obtained in these different engine conditions are presented in Table 5.

**Table 5.** Engine operating parameters.

Engine Speed [min <sup>-1</sup> ]	Injection Pressure [Bar]	Injection Pulse [μs]	Injector Current [A]	Injector Voltage [V]
695	300	614	9.94	14.3
1000	470	855	12.93	14.2
1500	630	1200	17.20	14.2
2000	860	1470	21.47	14.2
2500	1030	1665	25.74	14.2
3000	1160	1800	30.01	14.0

A test plan based on the behaviour of the injection map of the electronic control system of the 4JJ1 engine was carried out to generate a more reliable data acquisition and to ensure that the data from the injection bench were within the ideal working range of the vehicle, which is detailed in Table 6. It should be noted that this plan was applied in each nozzle, and for each time of energization, seven different pressures were used, resulting in a total of 210 tests carried out in each nozzle.

**Table 6.** Test plan.

Number Test	Pressure [MPa]	Energy Time [μs]
5	27–33	614
5	44–50	855
5	60–66	1200
5	83–89	1470
5	100–106	1665
5	113–119	1800

The modelling of the nozzle geometry was developed, defining the physical parameters, especially the number and dimensions of the hole diameters. This procedure was performed using a 20× magnification microscope with ToupView software (version 4.11). In this context, 4 different nozzles designed for the Denso 8-98011604 injector were examined and analysed. The detailed characteristics of these nozzles are listed in Tables 7 and 8, so their visual representations can be found in Figures 2 and 3. This approach to nozzle identification allows for an accurate assessment of the impact on spray behaviour and provides the opportunity to continually improve associated processes.

**Table 7.** Injector characteristics.

Denomination	Value	Units
Injector manufacturer	Denso	-
Model	8-98011604	-
Inductance	100 < I < 1200 H	Henry
Nozzle	8	Holes
Hole diameter	145.98	μm
Average injection flow	300	mm <sup>3</sup> /h
Return flow	82.5	mm <sup>3</sup> /h
Work pressure	25 < P <sub>inj</sub> < 150	MPa
Weight	689	g

**Table 8.** Nozzle characteristics.

Nozzle	Number of Holes	Diameter [μm]
1	5	209.8 ≈ 210
2	8	123.87 ≈ 124
3	8	145.98 ≈ 146
4	6	184.27 ≈ 184

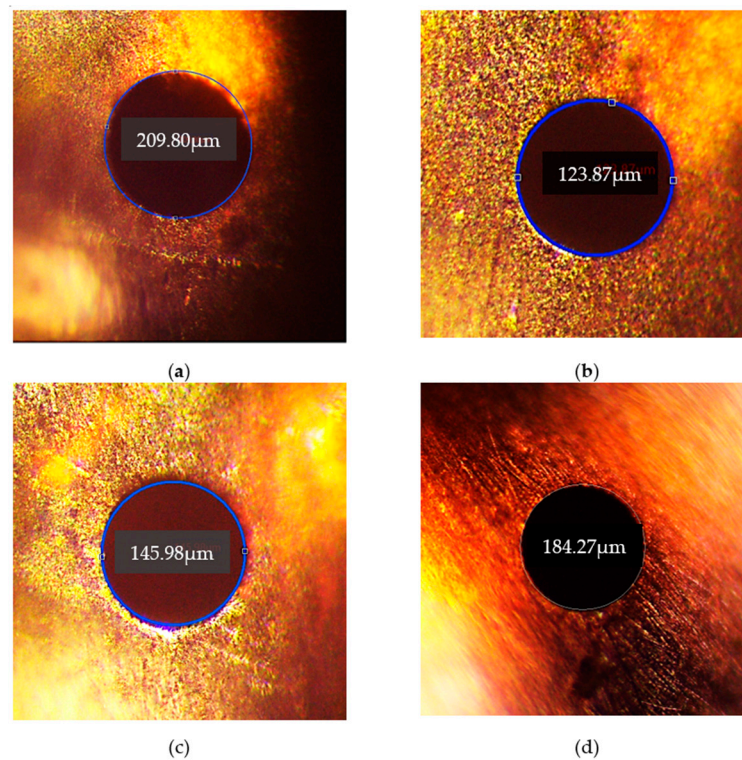


**Figure 2.** Diameters of the holes of the nozzles used. (a) Diameter of nozzle number 1; (b) diameter of nozzle number 2; (c) diameter of nozzle number 3; and (d) diameter of nozzle number 4.

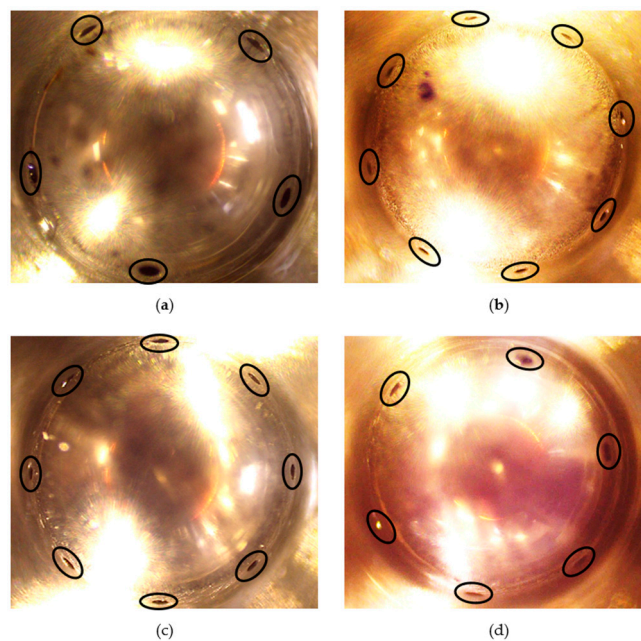


**Figure 3.** Number of nozzle holes used in (a) nozzle 1; (b) nozzle number 2; (c) nozzle number 3; and (d) nozzle number 4.

In the development of the 0D models in this section, the model of Equation (1) was used. This model is based on the calculation of the injection rate of the mass injected each time to analyse the injection behaviour (mass flow). From this same equation, two models were developed, one for the mass flow rate and one for the volumetric flow rate, defined as the volume of fluid passing through a given surface at each time (volumetric flow rate).

The flow measurement bench also provides the total mass of fuel, so the total mass flow rate can be determined.

The 0D model allows for obtaining the injection rate curve based mainly on fluid dynamics, taking as calculation variables the volumetric flow, injection pressure, injector opening time, and mass of the injected fuel. This study is based on the work carried out by Soriano et al. [18], where the mathematical model used allowed for obtaining the values necessary to model the behaviour of the injection rate using the following equation:

$$\dot{m}_f = C_d A_0 \sqrt{2(p_{inj} - p_{back}) \rho_f} \quad (1)$$

where  $C_d$  is the discharge coefficient (dimensionless),  $A_0$  represents the area of the fuel outlet of the nozzle ( $\text{mm}^2$ ),  $p_{inj}$  is the injection pressure (MPa),  $p_{back}$  refers to the pressure in the environment where the fuel is injected (MPa), and the fuel density is denoted as,  $\rho_f$  ( $\frac{\text{mg}}{\text{mm}^3}$ ).

### 2.3. Data Processing

Once the data from the test bench for diesel injectors were obtained, the software (Matlab 2023 and Minitab 17) were used for the data tabulation and prediction of the mathematical model for the Rate of Injection fuel (RoI<sub>m</sub>) curve, which was plotted to facilitate the analysis of the behaviour of the injection rate.

A curvature change analysis was performed in the software matrix laboratory (Matlab) for the behaviour of the rate and mass flow for time to proceed to performing a Multivariate Analysis of Variance (MANOVA), which provided a regression analysis and analysis of variance for multiple dependent variables by one or more covariates or factor variables.

Figure 4 describes the analytical experimental methodological process according to the different nozzles and tests.

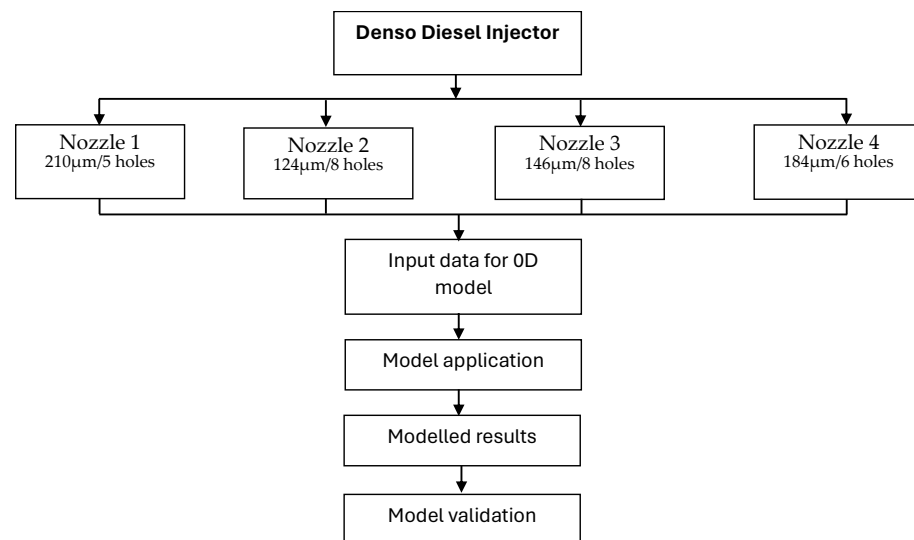


**Figure 4.** Methodological diagram.

## 3. Results

### 3.1. Volumetric Flow Rate and Mass Fuel

During the tests carried out on the diesel injector diagnostic bench, the values of the volumetric flow rate and mass of fuel injected for each energization time were registered. These values were obtained by adjusting the rotation speed of the high-pressure pump on the test bench (at identical revolutions of the vehicle engine), setpoint injection pressure, and pulse width. It should be noted that the tests were carried out with 3 MPa above and below the reference value of the setpoint injection pressure in each work condition,

as shown in Table 7, concerning which, an interpolation is made of the averages resulting from the tests carried out for the measurement of the mass of fuel injected for both fuels.

In addition, it could be noted that, when the tests were performed with the lowest pressure ranges, according to Table 5, the injector with nozzle 1 did not open, and this was assumed to be due the pressure characteristics of the internal spring, which means that the working ranges for low pressures with diesel in the tests generated non-efficient work.

In Figure 5, the behaviour of the flow and mass of the Viscor 1 (Fuel 1) provided with the bank of diesel injectors is shown. Both parameters were distributed based on the reference pressure obtained from the test vehicle and the nozzle used. In addition, the volumetric flow and amount of fuel injected at different pressures and pulses corresponding to the established work regimes presented in Tables 1 and 2 of the annexes are displayed.

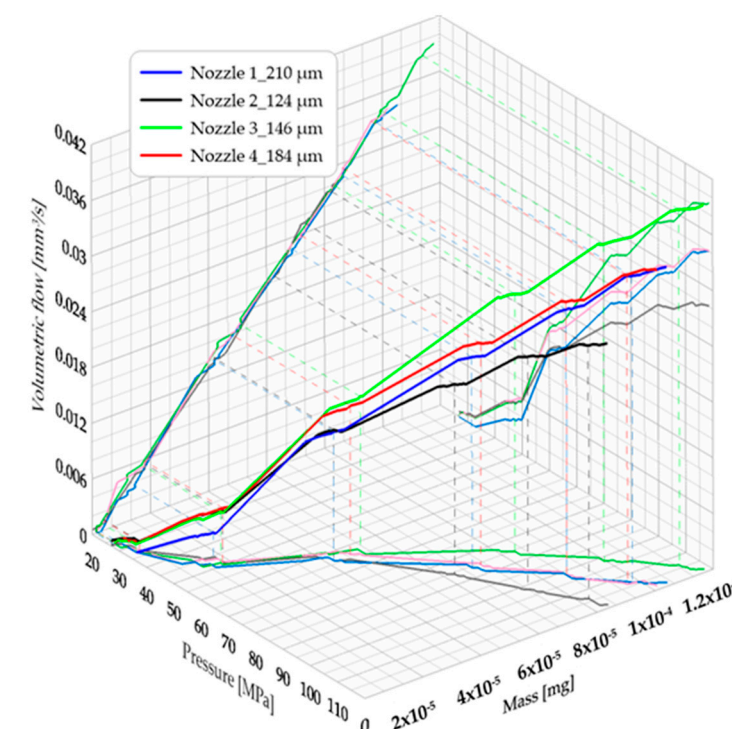


**Figure 5.** Volumetric flow of Viscor as a function of injection pressure.

The results shown in Figures 5 and 6 reflect the use of two types of fuel: Viscor (Fuel 1) and diesel (Fuel 2), respectively. These experiments were developed using four nozzles, whose geometry was previously characterised. Each solid intense colours indicated the projection in 3D of the results with each nozzle geometry. The lines with toned down colours correspond to the 2D projection of these results. This method aims to analyse and compare the performance of the fuels with different configurations of nozzles, allowing for a more complete evaluation of their behaviour under specific injection conditions.

For diesel fuel (Fuel 2), it should be noted that the operating parameters and nozzles used remained the same as those applied for Viscor fuel (Fuel 1). Figure 6 shows how the injected fuel's mass and flow values were obtained. As was commented previously, each solid intense colours indicated the projection in 3D of the results with each nozzle geometry. The lines with toned down colours correspond to the 2D projection of these results. These data were collected across a variety of usage patterns covering the operating conditions and analysed with the four selected nozzles to ensure a proper data comparison. This methodological approach increased coherence in the comparative analyses between the two fuels and the four nozzles, contributing to a better understanding of their behaviour in terms of mass and flow under controlled conditions.

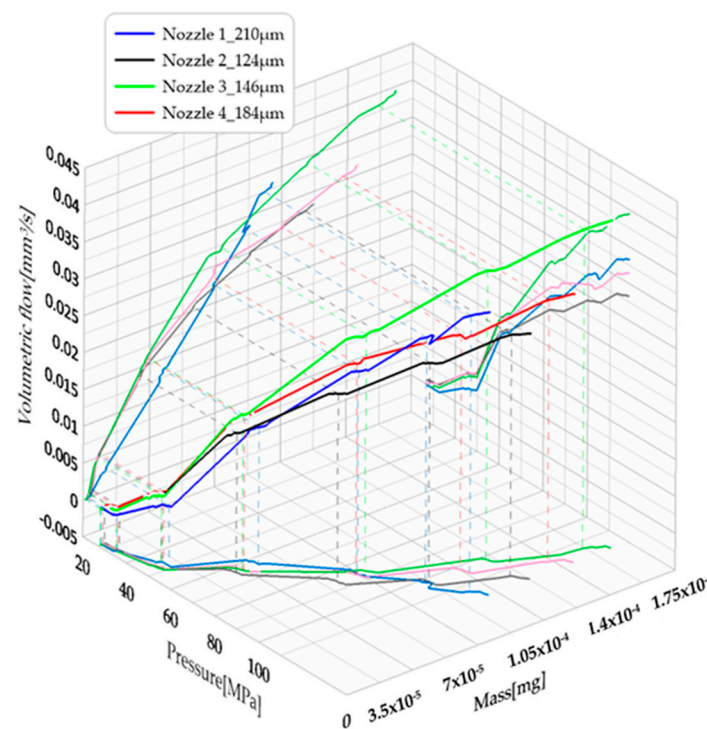


Figure 6. Volumetric flow of diesel as a function of injection pressure.

Due to the properties of the Viscor fuel, we observe in Figure 6 that the values achieved in both mass and volumetric flow were higher because its viscosity and density are lower in conditions of higher pressure and generate greater fuel deliveries. The volumetric flow stability was more linear in Viscor fuel than in diesel (shown in Figure 6).

### 3.2. Calculated RoI Data

Injection rate calculations were performed using Equation (1), using the flow obtained from the test bench and translated to the total mass of injection  $\dot{m}_f$  data collected during on-site testing (Figure 6). This process ensured the veracity of the measurement for all variables and avoided measurement errors. A relationship of units is required to ensure the accuracy of the results, allowing for a reliable comparison and analysis. The 0D model for calculating the RoI suggests the use of physical variables such as injection pressure, nozzle geometry, and properties of fuel such as density, and these parameters are applied mainly in Equation (1). Therefore, the injection rate for Viscor fuel (Fuel 1) was calculated with the equation, based on the flow and mass data presented in Table 9, the fuel density values detailed in Table 1, and the characterization of the nozzles shown in Table 8. Table 9 shows the volumetric flow values divided into two groups for each nozzle: the results obtained from the previously measured fuel flow and mass.

Table 9. Details of the variables of Equation (3).

Variables	Variable	Units
$\dot{m}_f$	RoI <sub>m</sub>	$\frac{\text{mg}}{\text{s}}$
$n$	Engine speed	$\text{min}^{-1}$
$p_{inj}$	Pressure	MPa
$m$	Mass fuel	mg
$A$	Area	$\text{mm}^2$
$\mu_f$	Kinematic viscosity	$\frac{\text{mm}^2}{\text{s}}$

The RoI calculations for diesel fuel (Fuel 2) were carried out in the same way as those for Viscor fuel (Fuel 1). Table 9 shows the injection rate values for the flow rate and mass injected in each work cycle. On the other hand, Figure 7a is a 3D graph, where the x-axis is the injection pressure, the y-axis is the calculated  $RoI_m$ , and the z-axis is the fuel flow rate. The same happens with Figure 7b, and the difference is that here the  $RoI_m$  calculated based on the mass is presented. The lines coloured have the same meaning than in the Figures 5 and 6.

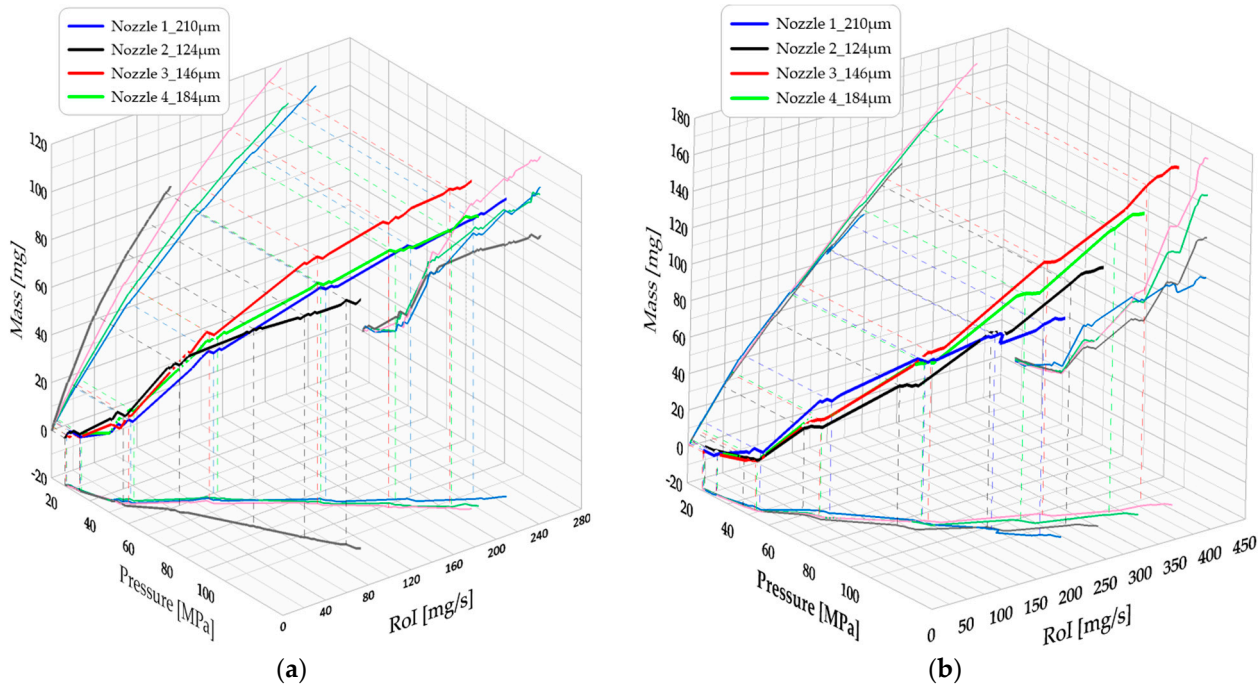


**Figure 7.** (a) Behaviour of the RoI calculated for Viscor fuel and (b) behaviour of the RoI calculated for diesel fuel.

### 3.3. Results of Multiple Regression

#### 3.3.1. Multiple Regression Model for $RoI_m$

The model equation is shown below:

$$\begin{aligned} \dot{m}_f = & -(1.17 \cdot 10^{-4}) - (1 \cdot 10^{-6}) p_{inj} + (3 \cdot 10^{-7}) m - (1.23 \cdot 10^{-4}) A \\ & + (9.2 \cdot 10^{-5}) \mu_f + (2 \cdot 10^{-6}) n \times A + (1 \cdot 10^{-6}) p_{inj} \times \mu_f \\ & - (1.2 \cdot 10^{-5}) m \times A - (1 \cdot 10^{-6}) m \times \mu_f - (4.76 \cdot 10^{-4}) A \times \mu_f \end{aligned} \quad (2)$$

A mathematical model was used to calculate the  $RoI_m$  based on the mass injected in each work cycle considering five fundamental variables detailed in Table 8.

The unit of the described model is  $\frac{mg}{s}$ , which allows us to correlate this equation with Equation (1) proposed by Soriano [18].

It should be noted that the area was calculated for the number of nozzle holes and their diameters, as shown in Equation (3).

$$A = \frac{\pi}{4} \times d^2 \times n_{holes} \quad (3)$$

This model had a regression of 99.56% of the variance, which indicates that the validation model presented had a high assertiveness with an error factor of less than 1%, which allowed for the calculation of the  $RoI_m$  for the mass of the fuel.

Figure 8a shows the behaviour of the incidence of each variable presented in the correlation model for the variations or fluctuations in the data measured during each test,

denoting that the most representative variable was the viscosity of the fuel, and Figure 8b shows the behaviour of the incidence of each variable presented in the correlation model for the importance of each variable for the use of Equation (3), noting that the variables with the highest representativeness were injection pressure and engine speed.

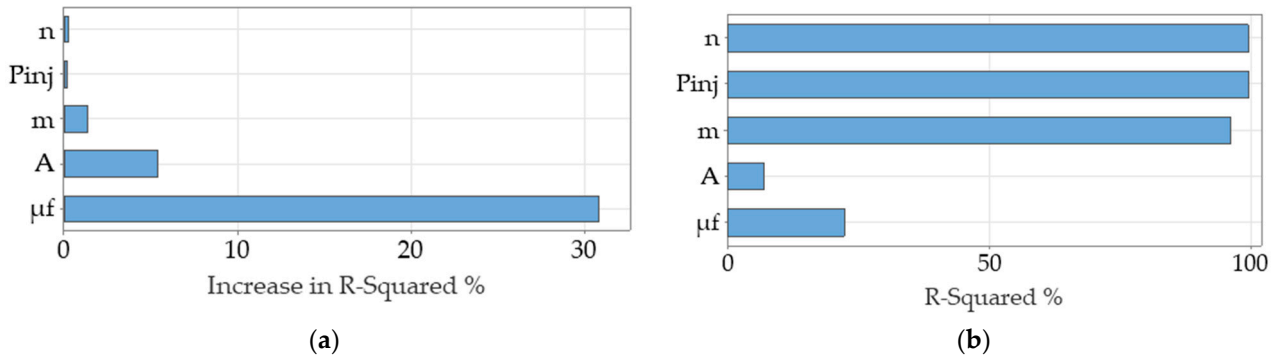


Figure 8. Representativeness (a) and incidence (b) of variables in Equation (3).

### 3.3.2. Multiple Regression Model for Fuel Mass Flow

The model equation is shown below:

$$\begin{aligned}
 RoI_{Flow} = & -(2.36 \cdot 10^{-2}) + 3.6 \cdot 10^{-5} * n - (3.522 \cdot 10^{-3}) P_{inj} + (3.135 \cdot 10^{-3}) m \\
 & + (0.376) A + (2.808 \cdot 10^{-2}) \mu_f + (2.7 \cdot 10^{-5}) P_{inj}^2 - (3 \cdot 10^{-6}) m^2 \\
 & - (2.886) A^2 - (1 \cdot 10^{-6}) \times n \times P_{inj} + (7.66 \cdot 10^{-4}) \times n \times A \\
 & - (2.5 \cdot 10^{-5}) \times n \times \mu_f + (6.74 \cdot 10^{-3}) P_{inj} \times A \\
 & + (4.79 \cdot 10^{-4}) P_{inj} \times \mu_f - (1.29 \cdot 10^{-2}) m \times A - (4.56 \cdot 10^{-4}) m \times \mu_f \\
 & - (0.15749) A \times \mu_f
 \end{aligned} \tag{4}$$

An equation was also modelled to calculate the RoI based on the flow rate value in each injection, considering the five fundamental variables detailed in Table 10.

Table 10. Details of variables in Equation (4).

Denomination	Variable	Units
$RoI_{Flow}$	Flow volume	$\frac{mm^3}{s}$
$n$	Engine speed	$min^{-1}$
$P_{inj}$	Pressure	MPa
$m$	Mass	mg
$A$	Area	$mm^2$
$\mu_f$	Kinematic viscosity	$\frac{mm^2}{s}$

The volumetric flow rate calculation for the injector and experimental results of the calibration injection bench is given in  $mm^3/s$ . This rate was calculated by comparing the mass of fuel injected with the volume delivered per unit time. This comparison was then compared with the manufacturer’s record to ensure accurate measurements.

This model had a regression of 99.42% of the variance, which indicates that the validation model presented had a high assertiveness with an error factor of less than 1%, which allowed for the calculation of the  $RoI_{Flow}$  for the fuel flow.

Figure 9a shows the behaviour of the incidence of each variable presented in the correlation model for the variations or fluctuations in the data measured during each test, denoting that the most representative variable was the viscosity of the fuel, and Figure 9b shows the behaviour of the incidence of each variable presented in the correlation model

for the importance of each variable for the use of Equation (4), denoting that the variables with the greatest representativeness were the injection pressure and the speed of the motor.

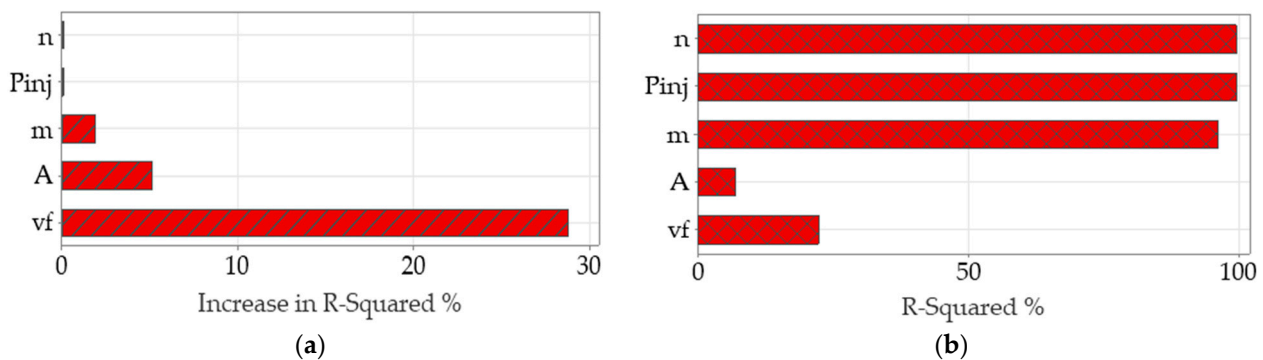


**Figure 9.** Representativeness (a) and incidence (b) of variables in Equation (4).

### 3.4. Discussion

As observed in the previous section, by varying the injector nozzle and the fuel used, the mass and flow values obtained varied, which directly influenced the behaviour of the injection rate and fuel spray. Firstly, by considering only the values obtained with the test bench in Figures 5 and 6, it was possible to determine the atomization of the fuel, since, by obtaining the same flow rate and mass with a higher injection pressure, the size of the drop would be smaller and, therefore, the distribution of the fuel in the combustion chamber would be better. From the comparison of the results obtained with the different configurations, a greater atomization was observed with the Viscor fuel (Fuel 1) using nozzle number 2 and starting at approximately 100 MPa, since the flow rate and mass reached were the same as those shown by nozzles 1 and 4 at a pressure of 80 MPa, occurring in the same way in diesel fuel (Fuel 2).

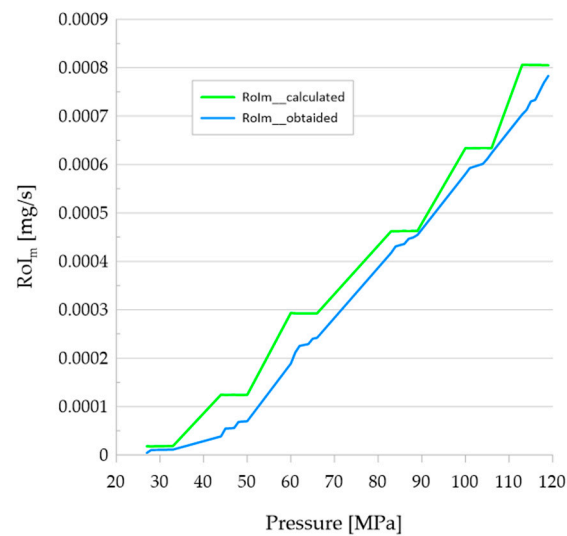
Based on the results presented in the previous section, the physical–chemical properties of the fuel played important roles in the behaviour of the injection rate. The maximum  $RoI_{Flow}$  reached (at a pressure of 119 MPa under a full load speed of  $3000 \text{ min}^{-1}$ ) was  $2.54 \times 10^{-6} \left[ \frac{\text{mm}^3}{\text{s}} \right]$  for the flow rate in nozzle 1. In the case of using fuel 2 (diesel) with the same nozzle and pressure, the maximum  $RoI_{Flow}$  reached was  $2.6 \times 10^{-7} \left[ \frac{\text{mm}^3}{\text{s}} \right]$ , with this fuel being denser and more viscous in the same temperature range. This behaviour was repeated with the three remaining nozzles.

On the other hand, by using the values obtained from the geometry in each nozzle, the influence of this on the injection rate was evident, since the fuel dispersion changed depending on the physical characteristics of the nozzle (as it was commented in Section 3.2). For both fuels,  $RoI_{Flow}$  increased with a smaller number of holes and a larger diameter, which indicates a larger cross-section. This behaviour was maintained with all nozzles.

## 4. Model Validation

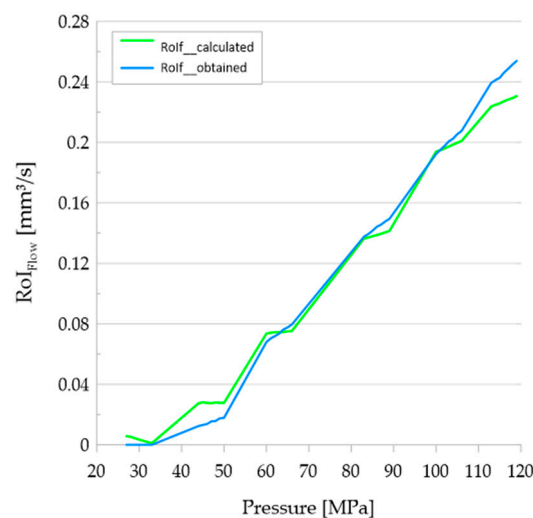
In this section, the model proposed for estimating the RoI (mass and flow) is validated with the experimental data shown in the previous section.

Figure 10 shows the comparison at an idle speed up to full load ( $RoI_m \left( \frac{\text{mg}}{\text{s}} \right)$ ) with nozzle 2, which allowed for predicting the diesel fuel consumption behaviour, focusing on the original injection map of diesel vehicles with current technologies. It should be noted that the behaviour of the original injection map was a progressive stepwise behaviour of the injected fuel mass, while the presented model was a stepwise type for the injection rate variation, denoting a more accurate delivery for the prediction of the injected fuel mass consumption at 96% with an error factor of  $\pm 4\%$ , discounting the stepwise step points and analysing the climb curve of the presented model with the measured data.



**Figure 10.** Comparison between  $RoI_m$  estimated and experimental obtained with diesel fuel.

Figure 11 illustrates a comparison of the increase in injection flow through the analysis of a prediction model of the injected volumetric flow rate ( $RoI_{Flow} \left( \frac{mm^3}{s} \right)$ ), which offers an advanced view of the behaviour of fuel consumption. This approach focuses on the original injection mapping of diesel vehicles to the operating parameters of the injector and CRDI pump calibration banks. In this case, the numerical equation presented fit more closely to the flow trend when nozzle 2 was used, which resulted in a notable improvement in the predictive capacity of the volume of fuel injected, considering variables such as pressure, number of holes, and the energization time of the Bosch injector.



**Figure 11.** Comparison between  $RoI_{Flow}$  estimated and experimental obtained with diesel fuel.

The test conditions were based on a gradual exponential progression, reaching a 93% approximation during the injection process up to the 110 MPa range and decreasing thereafter, with an error factor of 7% at the step points of the original injection map. This last value represents the maximum operating pressure in the working conditions of the vehicle, from which a decrease in pressure was observed.

Using the examples shown in Figures 10 and 11, other methods for evaluating the fuel injection rate and volumetric flow were explored. This was achieved by using a current injection system, which allows for a detailed description of the operating conditions. The objective is to improve the understanding of diesel fuel behaviour by controlling key

variables such as injection pressure, power delivery time, and the number of holes. These tools make it easy to predict and optimize performance, which is essential for checking and adjusting diesel injectors for optimal performance.

## 5. Conclusions

In this study, the influence of the number of holes and the difference in using a calibration fuel for conventional diesel fuel was evaluated to analyse the rate injection behaviour. The main conclusions obtained were:

- The nozzle with the highest fuel efficiency was the eight-hole nozzle with 124 microns, as it provided a better atomisation of the fuel with a lower injection rate value. In this way, it was possible to increase the injection pressure and decrease the pulse width or energisation time. In addition, by obtaining better atomisation, the air–fuel mixture would be more homogeneous, which would increase the combustion engine performance.
- If the cross-sectional area of the holes was smaller and the number of holes was greater, the fuel distribution in the engine would be much better and the injection rate would be adequate, as happened with nozzle number 2. On the other hand, nozzle number 1 (x number of holes and x diameter) was the least efficient in this case, since the values of flow rate, mass, and injection rate were the highest compared to the rest of the nozzles.
- When working nozzle 1 was used at a low engine speed and pressure (idle), injector 1 was not activated. This indicates that, to keep the vehicle running, the injection pressure, engine speed, and injection pulse would have to be increased, resulting in an even higher injection rate and fuel consumption.
- It is important to stress the importance of fuel viscosity characteristics, as these were shown to play important roles in the behaviour of the injection rate and, thus, fuel efficiency. This would extend engine life and reduce emissions to the environment.
- The two zero-dimensional models presented to predict the injection rate behaviour were close to the real behaviour of the 4JJ1 engine, so this will be very useful for future studies concerning injection rate behaviour.
- The importance of the zero-dimensional model used in the study should be emphasised, as this model facilitates data collection and shortens processing time. This is because, in most cases, physical data are used, which are often not very accessible.

**Author Contributions:** Conceptualization, E.V.R.-R., K.M.-C., J.A.S., R.G.-C.; methodology, E.V.R.-R., J.L.-L., J.A.S., R.G.-C.; software, E.V.R.-R., J.A.S.; validation, E.V.R.-R.; formal analysis, E.V.R.-R., K.M.-C., R.G.-C.; investigation, E.V.R.-R., K.M.-C.; resources, J.A.S.; data curation, E.V.R.-R. and J.A.S.; writing—original draft preparation, E.V.R.-R., J.A.S., R.G.-C.; writing—review and editing, E.V.R.-R., J.A.S., R.G.-C.; visualization, E.V.R.-R., J.A.S.; supervision, E.V.R.-R., J.A.S., R.G.-C.; project administration, E.V.R.-R.; funding acquisition, E.V.R.-R. All authors have read and agreed to the published version of the manuscript.

**Funding:** This research was funded by (i) the government of Castilla-La Mancha community to the project ASUAV, Ref. SBPLY/19/180501/000116, and (ii) Contribution from the national project (PID2020-118387RB-C32).

**Data Availability Statement:** The author declare the availability of the data and authorship of the data.

**Conflicts of Interest:** The authors declare no conflict of interest.

## References

1. Yu, H.; Liu, Y.; Li, J.; Ma, K.; Liang, Y.; Xu, H. Investigations on Fuel Consumption Characteristics of Heavy-Duty Commercial Vehicles under Different Test Cycle. *Energy Rep.* **2022**, *8*, 102–111. [[CrossRef](#)]
2. Liu, J.; Feng, L.; Wang, H.; Zheng, Z.; Chen, B.; Zhang, D.; Yao, M. Spray Characteristics of Gasoline/PODE and Diesel/PODE Blends in a Constant Volume Chamber. *Appl. Therm. Eng.* **2019**, *159*, 113850. [[CrossRef](#)]

3. Conway, G.; Joshi, A.; Leach, F.; García, A.; Senecal, P.K. A Review of Current and Future Powertrain Technologies and Trends in 2020. *Transp. Eng.* **2021**, *5*, 100080. [[CrossRef](#)]
4. Oh, J.; Oh, S.; Kim, C.; Lee, S.; Lee, S.; Jang, H.; Lee, J. Effect of Multi-Angle Diesel Injector Nozzle on Emission and Efficiency of Natural Gas/Diesel Dual-Fuel Combustion in Compression Ignition Engine. *Fuel* **2022**, *316*, 123442. [[CrossRef](#)]
5. Panda, K.; Ramesh, A. Diesel Injection Strategies for Reducing Emissions and Enhancing the Performance of a Methanol Based Dual Fuel Stationary Engine. *Fuel* **2021**, *289*, 119809. [[CrossRef](#)]
6. He, X.; Xu, K.; Xu, Y.; Zhang, Z.; Wei, W. Effects of Nozzle Diameter on the Characteristic Time Scales of Diesel Spray Two-Stage Ignition under Cold-Start Conditions. *Fuel* **2023**, *335*, 126700. [[CrossRef](#)]
7. Sujesh, G.; Ramesh, S. Modeling and Control of Diesel Engines: A Systematic Review. *Alex. Eng. J.* **2018**, *57*, 4033–4048. [[CrossRef](#)]
8. Praveena, V.; Leenus Jesu Martin, M.; Varuvel, E.G. Combined Effects of Nozzle Hole Variation and Piston Bowl Geometry Modification on Performance Characteristics of a Diesel Engine with Energy and Exergy Approach. *J. Clean. Prod.* **2022**, *375*, 133946. [[CrossRef](#)]
9. Atac, O.F.; Lee, S.; Moon, S. Development of Simplified Model for Injection Rate Prediction of Diesel Injectors during Transient and Steady Operation. *Fuel* **2022**, *324*, 124655. [[CrossRef](#)]
10. Mohan, B.; Yang, W.; Chou, S.K. Fuel Injection Strategies for Performance Improvement and Emissions Reduction in Compression Ignition Engines—A Review. *Renew. Sustain. Energy Rev.* **2013**, *28*, 664–676. [[CrossRef](#)]
11. Ishak, M.H.H.; Ismail, F.; Mat, S.C.; Abdullah, M.Z.; Abdul Aziz, M.S.; Idroas, M.Y. Numerical Analysis of Nozzle Flow and Spray Characteristics from Different Nozzles Using Diesel and Biofuel Blends. *Energies* **2019**, *12*, 281. [[CrossRef](#)]
12. Vera-Tudela, W.; Haefeli, R.; Barro, C.; Schneider, B.; Boulouchos, K. An Experimental Study of a Very High-Pressure Diesel Injector (up to 5000 Bar) by Means of Optical Diagnostics. *Fuel* **2020**, *275*, 117933. [[CrossRef](#)]
13. Ni, P.; Xu, H.; Zhang, Z.; Zhang, X. Effect of Injector Nozzle Parameters on Fuel Consumption and Soot Emission of Two-Cylinder Diesel Engine for Vehicle. *Case Stud. Therm. Eng.* **2022**, *34*, 101981. [[CrossRef](#)]
14. Payri, R.; Bracho, G.; Soriano, J.A.; Fernández-Yáñez, P.; Armas, O. Nozzle Rate of Injection Estimation from Hole to Hole Momentum Flux Data with Different Fossil and Renewable Fuels. *Fuel* **2020**, *279*, 118404. [[CrossRef](#)]
15. Rojas-Reinoso, V.; Duque-Escobar, S.; Guapulema-Guapulema, C.; Soriano, J.A. Study of the Variation of Fuel Pressure to Improve Spraying and the Range of the Injection Jet. *Energies* **2023**, *16*, 5472. [[CrossRef](#)]
16. Safiullah; Chandra Ray, S.; Nishida, K.; McDonell, V.; Ogata, Y. Effects of Full Transient Injection Rate and Initial Spray Trajectory Angle Profiles on the CFD Simulation of Evaporating Diesel Sprays—Comparison between Singlehole and Multi Hole Injectors. *Energy* **2023**, *263*, 125796. [[CrossRef](#)]
17. Yao, C.; Geng, P.; Yin, Z.; Hu, J.; Chen, D.; Ju, Y. Impacts of Nozzle Geometry on Spray Combustion of High Pressure Common Rail Injectors in a Constant Volume Combustion Chamber. *Fuel* **2016**, *179*, 235–245. [[CrossRef](#)]
18. Soriano, J.A.; Mata, C.; Armas, O.; Ávila, C. A Zero-Dimensional Model to Simulate Injection Rate from First Generation Common Rail Diesel Injectors under Thermodynamic Diagnosis. *Energy* **2018**, *158*, 845–858. [[CrossRef](#)]
19. Luo, T.; Jiang, S.; Moro, A.; Wang, C.; Zhou, L.; Luo, F. Measurement and Validation of Hole-to-Hole Fuel Injection Rate from a Diesel Injector. *Flow. Meas. Instrum.* **2018**, *61*, 66–78. [[CrossRef](#)]
20. Rojas-Reinoso, V.; Mata, C.; Soriano, J.A.; Armas, O. Zero-Dimensional Modeling of the Rate of Injection with a Diesel Common Rail System Using Single-Hole Nozzles with Neat Low-Carbon Fuels. *Appl. Sci.* **2024**, *14*, 2446. [[CrossRef](#)]
21. Mata, C.; Rojas-Reinoso, V.; Soriano, J.A. Experimental Determination and Modelling of Fuel Rate of Injection: A Review. *Fuel* **2023**, *343*, 127895. [[CrossRef](#)]
22. Salvador, F.J.; Gimeno, J.; Martín, J.; Carreres, M. Thermal Effects on the Diesel Injector Performance through Adiabatic 1D Modelling. Part I: Model Description and Assessment of the Adiabatic Flow Hypothesis. *Fuel* **2020**, *260*, 116348. [[CrossRef](#)]
23. Zhang, T. An Estimation Method of the Fuel Mass Injected in Large Injections in Common-Rail Diesel Engines Based on System Identification Using Artificial Neural Network. *Fuel* **2022**, *310*, 122404. [[CrossRef](#)]
24. Kim, J.; Lee, J.; Kim, K. Numerical Study on the Effects of Fuel Viscosity and Density on the Injection Rate Performance of a Solenoid Diesel Injector Based on AMESim. *Fuel* **2019**, *256*, 115912. [[CrossRef](#)]
25. Zhai, C.; Jin, Y.; Nishida, K.; Ogata, Y. Diesel Spray and Combustion of Multi-Hole Injectors with Micro-Hole under Ultra-High Injection Pressure–Non-Evaporating Spray Characteristics. *Fuel* **2021**, *283*, 119322. [[CrossRef](#)]
26. Catania, A.E.; Finesso, R.; Spessa, E. Predictive Zero-Dimensional Combustion Model for Di Diesel Engine Feed-Forward Control. *Energy Convers. Manag.* **2011**, *52*, 3159–3175. [[CrossRef](#)]
27. Payri, R.; Molina, S.; Salvador, F.J.; Gimeno, J. A Study of the Relation between Nozzle Geometry, Internal Flow and Sprays Characteristics in Diesel Fuel Injection Systems. *KSME Int. J.* **2004**, *18*, 1222–1235. [[CrossRef](#)]
28. Rojas-Reinoso, V.; Alvarez-Loor, J.; Zambrano-Becerra, H.; Soriano, J.A. Comparative Study of Gasoline Fuel Mixture to Reduce Emissions in the Metropolitan District. *Sustainability* **2023**, *15*, 2921. [[CrossRef](#)]
29. AEADE. *BOLETÍN DE PRENSA Ventas de Vehículos-Resumen*; AEADE: Quito, Ecuador, 2023.

**Disclaimer/Publisher’s Note:** The statements, opinions and data contained in all publications are solely those of the individual author(s) and contributor(s) and not of MDPI and/or the editor(s). MDPI and/or the editor(s) disclaim responsibility for any injury to people or property resulting from any ideas, methods, instructions or products referred to in the content.